ELSEVIER
Chemical Engineering Journal 92 (2003) 141–150
Chemical Engineering Journal
www.elsevier.com/locate/cej

Study of the regeneration stage of the MTG process in a pseudoadiabatic fixed bed reactor

Andrés T. Aguayo*, Ana G. Gayubo, Javier Ereña, Raquel Vivanco, Javier Bilbao

Departamento de Ingeniería Química, Universidad del País Vasco, Apartado 644, 48080 Bilbao, Spain

Accepted 6 July 2002

Abstract

The regeneration stage of a catalyst (prepared based on an HZSM-5 zeolite) has been studied in the process of transformation of methanol into hydrocarbons in a fixed bed reactor. The simulation of the operation requires knowledge of the longitudinal profile of coke content in the reactor at the end of the reaction stage. Longitudinal profiles of temperature, coke content and activity during the regeneration are calculated by solving the energy conservation equation in the reactor together with the kinetic equation for coke combustion and with the kinetic equation for reactivation (activity–coke content relationship). The results of the simulation have been experimentally verified in a laboratory unit provided with a pseudoadiabatic fixed bed reactor.

Keywords: Regeneration stage; HZSM-5 zeolite; Fixed bed reactor

1. Introduction

In spite of the good performance of the catalyst (prepared based on a ZSM-5 zeolite) against deactivation and of the fact that the operating conditions are chosen in order to attenuate this problem, deactivation by coke is relatively rapid in the MTG (methanol to gasoline) process and, consequently, the catalyst must be periodically regenerated by coke combustion [1–3].

Taking into account the importance of the regeneration stage in the yields and the economy of the MTG process, the aim of this paper is to study the design of this stage by incorporating recent advances in the kinetic modeling of regeneration by coke combustion [4–7]. The simulation results have been verified by operating in a laboratory unit in pseudoadiabatic regime.

The aim of the design of the regeneration stage is to ascertain the effect of the regeneration conditions on the evolution of the catalyst activity profile along the reactor with combustion time. Thus, the time required for total or partial recovery of activity in the reactor will be determined. It must be taken into account that, in an operation carried out in reaction–regeneration cycles, the optimum strategy does not necessarily imply total regeneration of the catalyst [8–11]. Furthermore, as coke combustion is an exothermal reaction and the reactor is adiabatic, the evolution of the temperature profile with time must be determined in order to avoid (by choosing the operating conditions) the deterioration by temperature of the active sites of the catalyst (irreversible deactivation).

Since the pioneering papers of Van Deempter [12,13] and Johnson et al. [14] on the design of the regeneration stage in adiabatic reactors, the real circumstances of this stage have been taken into account in studies in this field, as are the consideration of the longitudinal profile of coke content [15,16], the different combustion of coke constituents (hydrogen and carbon) [16–18] and the effect of other factors (linear velocity of the combustion gas, oxygen content, temperature of the inlet gas) [19]. Santamaría et al. [20] have studied the strategies involved in changing the operating conditions with time and their effect on the evolution of coke and temperature profiles.

It is noteworthy that most of the studies in the literature correspond to metallic catalysts. Nevertheless, studies of this nature are even more important in certain processes, such as the MTG carried out on acidic catalysts, because they are of lower hydrothermal stability than the metallic catalysts.

2. Experimental

2.1. Equipment

The reaction equipment used in the pseudoadiabatic regime operation has already been described [21]. The

---

* Corresponding author. Tel.: +34-94-601-2580; fax: +34-94-464-8500.
E-mail address: iqpagura@lg.ehu.es (A.T. Aguayo).

1385-8947/02/$ – see front matter © 2002 Elsevier Science B.V. All rights reserved.
PII: S1385-8947(02)00187-0

Nomenclature

a	catalyst activity at the beginning of regeneration
a_0	catalyst activity subsequent to the regeneration stage
C_c, $C_{c,ext}$, C_{cT}	coke content in the catalyst, external coke content and total coke content, respectively, based on coke-free catalyst (wt.%)
c_p	average heat capacity of the bed ($J\,kg^{-1}\,K^{-1}$)
C_{pg}	average heat capacity of the gaseous stream ($J\,mol^{-1}\,K^{-1}$)
C_{pi}, $C_{p\,in}$	heat capacity of i combustion gas and of the inert gas ($J\,mol^{-1}\,K^{-1}$)
c_{pw}	heat capacity of the reactor wall ($J\,kg^{-1}\,K^{-1}$)
F_d	catalyst dilution factor ((kg of bed) (kg of catalyst)$^{-1}$)
F_{in}	molar flow of the inert gas in the regeneration stage ($mol\,s^{-1}$)
F_{Mo}	mass flow of the methanol in the feed ($kg\,s^{-1}$)
$-\Delta H_c$	coke combustion heat (J (kg of coke)$^{-1}$)
K_a	effective thermal conductivity in the axial direction ($J\,s^{-1}\,m^{-2}\,K^{-1}$)
k_r	kinetic constant for coke combustion ($Pa^{-1}\,s^{-1}$)
k_1–k_4	kinetic constant for the steps corresponding to Eqs. (9)–(12)
M_c	molecular weight of coke ($kg\,mol^{-1}$)
n_h	H/C atomic ratio
P_{CO}, P_{O_2}	partial pressure of carbon monoxide and oxygen, respectively (Pa)
Q_{air}, Q_{N_2}	flow-rates of air and nitrogen, respectively ($cm^3\,s^{-1}$)
r_c	coke combustion rate ((kg of coke) (kg of catalyst)$^{-1}$ s^{-1})
R_e, R_i	external and internal radius of the reactor, respectively (m)
t	coke combustion time (s)
T	temperature (K)
T_e	temperature on the outside of the reactor (K)
T_0	temperature at the bed inlet (K)
U	global heat transfer coefficient ($J\,s^{-1}\,m^{-2}\,K^{-1}$)
W	catalyst weight (kg)
x_i, x_{in}	molar fraction of each combustion gas and of the inert gas by molar unit of the inert gas, respectively
X_i	mass fraction of each i product lump by mass unit of organic components
X_{Wo}	water/organic component mass ratio in the feed
z	reactor length (m)

Greek letters

β	molar ratio CO/CO_2
ρ	apparent catalyst density ($kg\,m^{-3}$)
ρ_w	density of the reactor wall ($kg\,m^{-3}$)

reactor (Fig. 1) is made of 316 stainless steel and has a 0.028 m internal diameter, 0.032 m external diameter and is 1 m in length (including the preheating zone of 0.235 m in length and 0.034 m internal diameter). The catalyst bed is located on a distributor plate with orifices of 1.5 μm diameter. Due to the fact that the reaction is exothermal, and in order to limit the temperature in the reactor, the catalyst is diluted with 90 wt.% alumina, which has been previously calcined at 1273 K in order to eliminate the residual activity that may catalyze certain steps in the MTG process. The length of the catalytic bed is 0.30 m.

The reactor is surrounded by a stainless steel encasing containing six electric resistances placed in succession. The first one is of 1000 W and is located in the preheating zone. The other five are of 750 W each. The role of these resistances, which are individually controlled, is to maintain a pseudoadiabatic regime by compensating the heat loss across the external wall of the encasing. Prior to the reaction, and by feeding a stream of inert gas, the power required in each one of the resistances for compensating the heat losses is established, so that uniform temperature is reached. This power is maintained throughout the runs.

In the feed preheating zone there is a device for rapidly correcting the reactor inlet temperature. It consists of a tube, with pressurized air as cooling fluid, which is activated when temperature is 2 K above the set point. The reactor is provided with K thermocouples which are set 0.05 m apart. At each longitudinal position there are three thermocouples for measuring the temperature at three radial positions in the bed (axis, intermediate zone and wall). The products pass

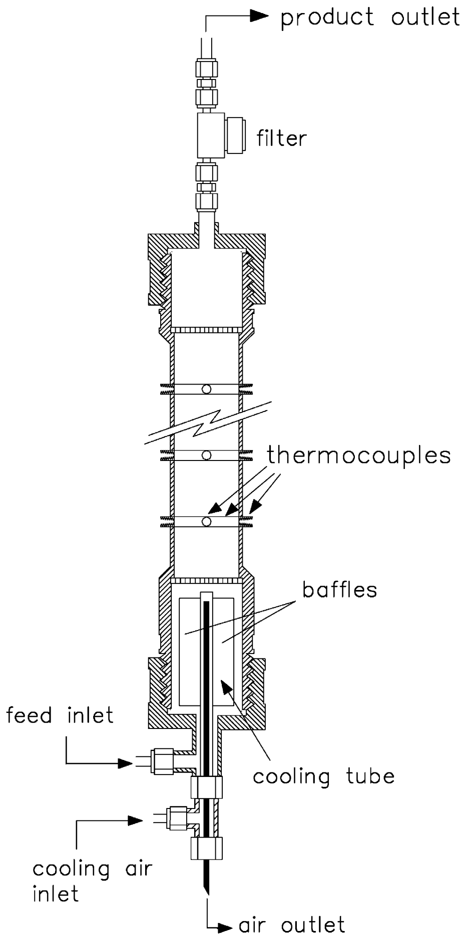

Fig. 1. Reactor scheme.

Table 1
Properties of HZSM-5 zeolite and catalyst

	HZSM-5 zeolite	Catalyst[a]
Si/Al ratio	24	
Bronsted/Lewis ratio	2.9	
Crystallinity (%)	97	
Crystal size (mm)	6.3	
Particle size (mm)		0.3–0.5
Apparent density ($g\,cm^{-3}$)	0.94	1.21
BET surface area ($m^2\,g^{-1}$)	420	124
Pore volume ($cm^3\,g^{-1}$)	0.65	0.43
Micropore volume ($cm^3\,g^{-1}$) (99% of diameter <0.7 nm)	0.17	
Pore volume distribution of the catalyst (vol.%)		
$d_p < 10^{-3}$ µm	8.1	
$d_{\text{<RM>p</RM>}} = 10^{-3}$–$10^{-2}$ µm	14.7	
$d_{\text{<RM>p</RM>}} = 10^{-2}$–2 µm	77.2	
	NH_3	*tert*-Butylamine
Zeolite acidity measurements		
Total acidity (mmol of base g^{-1})	0.51	0.46
Temperature peaks in the TPD (K)	695	577

[a] Composition: zeolite, 25 wt.%; bentonite, 30 wt.%; alumina, 45 wt.%.

through a 10-port valve that allows for a sample to be sent to the Hewlett-Packard 5890 Series II chromatograph. The feed–reaction–analysis system is controlled by a computer run by means of a program in FORTRAN.

Product separation is carried out using an arrangement of three columns: (1) semicapillary HP-1, of 0.53 mm diameter and 5.0 m length. It splits the sample into two fractions: (a) volatile (C_1–C_4) and polar (methanol, water and DME); (b) the remaining products. (2) Semicapillary SUPEL-Q Plot, of 0.53 mm diameter and 30.0 m length, for complete separation of volatile and polar components, which will be analyzed using TCD (thermal conductivity detector) and FID (flame ionization detector). (3) Capillary PONA of 0.20 mm diameter and 50.0 m length, for separation of the remaining products, which will be analyzed by FID.

A detailed identification of the components analyzed by chromatography was performed by means of GC–FT-IR (Hewlett-Packard 5890 II-Nicolet 740) and by means of GC–MS (Hewlett-Packard 5890 II-Engine from Hewlett-Packard). The identification of the components (isoparaffins, olefins, aromatics and naphthenes) was carried out using PIANO standard samples for chromatography from Air Liquide. The calibration of the areas corresponding to the chromatographic peaks was carried out using specific factors for each component. These factors were contrasted using commercial mixtures from Air Liquide and methanol–water mixtures at given proportions.

2.2. Catalyst

The ZSM-5 zeolite has been synthesized with a Si/Al ratio, Si/Al = 24, from sodium silicate, aluminum sulfate, and tetra-*n*-propylammonium bromide, and has been cation-exchanged to HZSM-5 by using ammonium nitrate. The method used has been detailed in a previous paper [22] following Mobil patents [23,24]. The zeolite has been subjected to an agglomeration process with bentonite (Exaloid), using fused alumina (Martinswerk) as inert charge. The properties of the HZSM-5 zeolite and catalyst are set out in Table 1. The Bronsted/Lewis ratio has been measured by FT-IR spectrometry from the intensity of the adsorption bands at 1550 and 1455 cm^{-1}. Prior to use, the catalyst is calcined at 843 K for 2 h, for the experimental results to be reproducible under reaction–regeneration cycles [25].

3. Kinetic modeling of the regeneration

In a previous paper [7] the kinetic tools required for designing the regeneration stage in an adiabatic fixed reactor have been obtained. Due to the fact that, in the regeneration by coke combustion in an adiabatic reactor, the longitudinal profile of temperature evolves with time, a reactivation equation as that used in an isothermal reactor is not sufficient for the design of the regeneration stage. In an isothermal reactor the activity recovered, a_0, is related to the combustion time, t_c, by means of the following empirical relationship:

$$
\begin{aligned}
a_0 = {} & 1-(1-a)\exp[-(1.38(\pm 0.112)\times 10^{-1}a \\
& -5.00(\pm 1.43)\times 10^{-3})t_c-(6.13(\pm 0.50) \\
& \times 10^{-4}-3.06(\pm 4,99)\times 10^{-3}a)t_c^2]
\end{aligned}
\qquad (1)
$$

The procedure followed for obtaining this equation and the physical meaning of its terms have already been explained [7]. Term a corresponds to the activity of the catalyst at the beginning of the regeneration stage. Consequently, this term depends on the experimental conditions of the reaction stage. Eq. (1) corresponds to the combustion of coke with air at 823 K, which is carried out subsequent to stripping with a N_2 stream at 823 K for 30 min. In this stripping process the coke structure is homogenized at all the positions of the reactor.

For the adiabatic reactor, an expression that relates the activity recovered to the coke content remaining in the catalyst is more suitable for the reactivation kinetics:

$$a_0 = \exp(-f_a C_c) \qquad (2)$$

where the term f_a is a function of the activity at the end of the reaction stage, a:

$$
\begin{aligned}
f_a = {} & -1.633(\pm 0.035)a^3+3.207(\pm 0.027)a^2 \\
& -2.306(\pm 0.019)a+0.798(\pm 0.010)
\end{aligned}
\qquad (3)
$$

This relationship was determined from those corresponding to $a_0 - t_c$, Eq. (1), and $C_c - t_c$, which is the kinetics for coke combustion. This kinetic equation has the following expression:

$$
\begin{aligned}
-\frac{dC_c}{dt} & = k_r C_c P_{O_2} \\
& = 1.16(\pm 0.35)\exp\left[\frac{-13\,800(\pm 120)}{T}\right] C_c P_{O_2}
\end{aligned}
\qquad (4)
$$

Furthermore, it has been proven that an amount of coke, whose content is $C_{c,ext}$, is externally deposited on the solid used for diluting the catalyst. This coke is different to that deposited in the crystalline structure of the catalyst and does not contribute to deactivation. It has been proven that the elimination of the external coke does not play any part in activity recovery.

The kinetic parameters for coke combustion in Eq. (4) were obtained by fitting the experimental data of weight loss rate, dC_c/dt, to this equation. This rate, was obtained in a thermogravimetric equipment by working under a programmed sequence of temperature–time [7]. Taking into account that the differences in the experimental results of combustion between samples of external and internal coke are small, the kinetic parameters in Eq. (4) correspond to samples taken from the whole catalytic bed and, consequently, are made up of internal and external coke. Consequently, Eq. (4) is used either for calculating the evolution of total coke content from the longitudinal profile of total coke in the reactor or for calculating the evolution of internal coke when its initial profile is known.

It is deduced from Eqs. (2) and (3) that, depending on the level of coke deposition, the catalyst recovers its activity in a different way when coke is burnt. In those bed zones where severe deactivation occurred, activity recovery is laborious, whereas for relatively high values of initial activity regeneration is efficient.

4. Simulation of the regeneration stage

The simulation of the regeneration stage consists in calculating the evolution with combustion time of the longitudinal profiles of temperature and coke in the reactor. This calculation is carried out by simultaneously solving the energy balance and the coke combustion kinetics. The activity profile is determined from that of internal coke, by means of Eq. (2).

In order to carry out these calculations, knowledge of coke content profile at the beginning of the regeneration stage is required. This profile is calculated by means of the activity–coke content relationship in the reaction stage [7]:

$$a = \exp[-(0.10C_c + 0.03C_c^2 - 0.01C_c^3)] \qquad (5)$$

This relationship has been determined experimentally by means of the results of activity and coke content at different longitudinal positions in the catalytic bed. The coke content was determined by combustion in a thermobalance (STD 2960 from TA Instruments) of deactivated catalyst samples taken at five longitudinal positions in the reactor. The activity values corresponding to the reactor positions at which the catalyst samples had been taken were calculated by means of a simulation program for the reaction stage, which has been described in detail in a previous work [26].

Furthermore, it has been determined that there is a relationship between external and internal coke content [7,27]:

$$C_{c,ext} = 6.39C_c^{0.18} \qquad (6)$$

Knowledge of external coke content is important due to the fact that, although it does not contribute to catalyst deactivation, it does make a major contribution to an increase in temperature in the bed during combustion and it must be taken into account in the energy conservation equation for the regeneration stage. This equation (considering the energy accumulation at the reactor wall), is

$$
\begin{aligned}
& (\pi(R_e^2-R_i^2)\rho_w c_{pw}+\pi R_i^2\rho c_p F_d)\frac{\partial T}{\partial t} \\
& \quad = (-\Delta H_c)r_c\rho\pi R_i^2-2\pi R_i U(T-T_e) \\
& \qquad -F_{in}C_{pg}\frac{\partial T}{\partial z}+\pi R_i^2 K_a\frac{\partial^2 T}{\partial z^2}
\end{aligned}
\qquad (7)
$$

The following considerations must be taken into account in Eq. (7): temperature is radially uniform at a given longitudinal position in the bed; the values of the global heat transfer coefficient and longitudinal heat dispersion are $U = 33\,\mathrm{J\,s^{-1}\,m^{-2}\,K^{-1}}$ and $K_a = 12\,\mathrm{J\,s^{-1}\,m^{-1}\,K^{-1}}$. These parameters have been determined experimentally by studying the heat transmission in the catalytic bed without reaction. For this purpose, the longitudinal profiles of temperature have been measured in the bed, by feeding an inert gas at a given temperature. U and K_a are the values that provide the best fitting of the experimental profiles to Eq. (7), without the term corresponding to the heat generated by reaction. The calculated values are different to those corresponding to the design of the reaction stage ($U = 2.0\,\mathrm{J\,s^{-1}\,m^{-2}\,K^{-1}}$ and $K_a = 0.4\,\mathrm{J\,s^{-1}\,m^{-1}\,K^{-1}}$), due to the fact that the average temperature in the regeneration stage is approximately 150 K higher than that corresponding to the reaction stage. The density changes due to temperature gradients and changes in composition are negligible. The transport coefficients are constant with both longitudinal position and temperature.

In Eq. (7) the term corresponding to coke combustion rate, r_c, includes the combustion of both the internal and external coke.

The average heat capacity of the combustion gases, C_{pg}, is determined by means of the contribution of both the individual combustion gases (O_2, CO, CO_2 and H_2O) and the inert gas (N_2):

$$C_{pg} = \sum_{i}^{n} x_i C_{pi} + x_{\mathrm{in}} C_{p\,\mathrm{in}} \tag{8}$$

where the heat capacity of each component is obtained from the literature [28].

The composition of the combustion gases is determined from the stoichiometry of the individual reactions:

$$\mathrm{C} + \tfrac{1}{2}\mathrm{O_2} \xrightarrow{k_1} \mathrm{CO} \tag{9}$$

$$\mathrm{C} + \mathrm{O_2} \xrightarrow{k_2} \mathrm{CO_2} \tag{10}$$

$$\mathrm{CO} + \tfrac{1}{2}\mathrm{O_2} \xrightarrow{k_3} \mathrm{CO_2} \tag{11}$$

$$\tfrac{1}{2}\mathrm{H_2} + \tfrac{1}{4}\mathrm{O_2} \xrightarrow{k_4} \tfrac{1}{2}\mathrm{H_2O} \tag{12}$$

Oxygen consumption is calculated by solving the following equations:

$$\begin{aligned} r_{O_2} &= -\frac{\mathrm{d}x_{O_2}}{\mathrm{d}t} \\ &= -\left(\frac{1}{2}k_1 - k_2 - \frac{1}{4}k_4 n_h\right) C_c P_{O_2} - \frac{1}{2}k_3 P_{CO} P_{O_2} \end{aligned} \tag{13}$$

$$r_{CO_2} = \frac{\mathrm{d}x_{CO_2}}{\mathrm{d}t} = k_2 C_c P_{O_2} + k_3 P_{CO} P_{O_2} \tag{14}$$

$$r_{CO} = \frac{\mathrm{d}x_{CO}}{\mathrm{d}t} = k_1 C_c P_{O_2} - k_3 P_{CO} P_{O_2} \tag{15}$$

$$r_{H_2O} = \frac{\mathrm{d}x_{H_2O}}{\mathrm{d}t} = \frac{1}{2}k_4 n_h C_c P_{O_2} \tag{16}$$

The kinetic constant k_1 and k_2 are calculated from the kinetic constant for coke combustion, k_r and from the value of the CO/CO_2 ratio, by means of the following expressions [18]:

$$k_1 = k_r \frac{\beta}{(\beta + 1) M_c} \tag{17}$$

where

$$\beta = \frac{\mathrm{CO}}{\mathrm{CO_2}}$$

$$k_2 = k_r \frac{1}{(\beta + 1) M_c} \tag{18}$$

From the experimental results obtained in different coke combustion runs, in which the composition of combustion gases with time was monitored by mass spectrometry, it has been determined that the CO/CO_2 ratio is very low for all the cokes studied and, consequently, a constant value has been taken, $\beta = 0.1$. On the other hand, for the H/C ratio a value of $H/C = 1$ has been taken, due to the fact that the values of this ratio determined by monitoring the combustion gases by mass spectrometry approximate this value. The value for the combustion enthalpy, $\Delta H_c = 30\,\mathrm{kJ/g_{coke}}$, has been determined by differential scanning calorimetry. These values for coke combustion parameters are similar to those previously obtained by Ortega et al. [5] for cokes subjected to a thermal treatment prior to combustion. For k_3 and k_4 the values determined by Arbel et al. [18] have been taken.

5. Experimental verification

The validity of the simulation program has been proven by comparing experimental results with those calculated for the operation in reaction–regeneration cycles. Table 2 shows the conditions of reaction and regeneration stages for two experimental systems (reaction–regeneration cycles) taken as an example for regenerator simulation. In the period of time between the stages of reaction and regeneration, a nitrogen stream circulates through the catalytic bed. This period

Table 2
Operating conditions in the reaction and regeneration, for two cases taken as an example for showing the regenerator simulation

Case	Reaction	Regeneration
1	T_0: 623 K X_{Wo}: 1 Time on stream: 13 h F_{Mo}: $1.04 \times 10^{-5}\,\mathrm{kg\,s^{-1}}$ Q_{N_2}: $2.31\,\mathrm{cm^3\,s^{-1}}$ W/F_{Mo}: 1602 $\mathrm{kg_{catalyst}\,s/kg_{MeOH}}$	T_0: 798 K Q_{air}: $3.58\,\mathrm{cm^3\,s^{-1}}$ Q_{N_2}: $3.55\,\mathrm{cm^3\,s^{-1}}$
2	T_0: 623 K X_{Wo}: 0 Time on stream: 6 h F_{Mo}: $2.08 \times 10^{-5}\,\mathrm{kg\,s^{-1}}$ Q_{N_2}: $2.31\,\mathrm{cm^3\,s^{-1}}$ W/F_{Mo}: 813.6 $\mathrm{kg_{catalyst}\,s/kg_{MeOH}}$	T_0: 798 K Q_{air}: $5.42\,\mathrm{cm^3\,s^{-1}}$ Q_{N_2}: $1.78\,\mathrm{cm^3\,s^{-1}}$

is required with the aim of homogenizing the coke. Thus, when the temperature rises from that of reaction to that of coke combustion (823 K), the coke undergoes an aging process in which its structure is modified by a reduction in the H/C ratio, and it is homogenized. Consequently, at the beginning of the regeneration coke has a similar H/C ratio in all its longitudinal positions in the reactor and thus the same combustion kinetics.

The experimental conditions of both cases of Table 2 have been established taking into account the temperature limitation in the reaction stage, whose maximum value is 723 K, because above this temperature and when water concentration in the reaction medium is high, the catalyst undergoes irreversible deactivation by dealumination of the HZSM-5 zeolite [29,30]. On the other hand, the maximum reactor temperature in the regeneration stage is 843 K, which is the temperature used in the thermal equilibration of the catalyst (final step in the preparation), and above which it undergoes an significant dealumination [25].

It has been proven that under these experimental conditions the catalyst totally recovers the activity when operation is carried out in reaction–regeneration cycles (10 cycles were performed).

Fig. 2 shows the longitudinal profiles of coke (internal or catalytic and external or outside the catalyst) in the reactor calculated at the beginning of the regeneration stage for both the cases displayed in Table 2. These profiles have been obtained by means of Eqs. (5) and (6), and from the corresponding activity profiles calculated by solving simultaneously the mass and energy conservation equations for the reactor together with the kinetic equation for deactivation, following the procedure detailed elsewhere [26]. The shape of the coke profiles in Fig. 2 has important consequences in the calculation of the temperature profile in the regeneration stage. It is observed in Fig. 2 that, for case 1 of Table 2, in which the methanol fed into the reactor is highly diluted with water, the longitudinal profile of coke in the reactor is more homogeneous than for case 2, corresponding to pure methanol in the feed. This difference leads to a more uniform temperature profile in the regeneration stage for case 1.

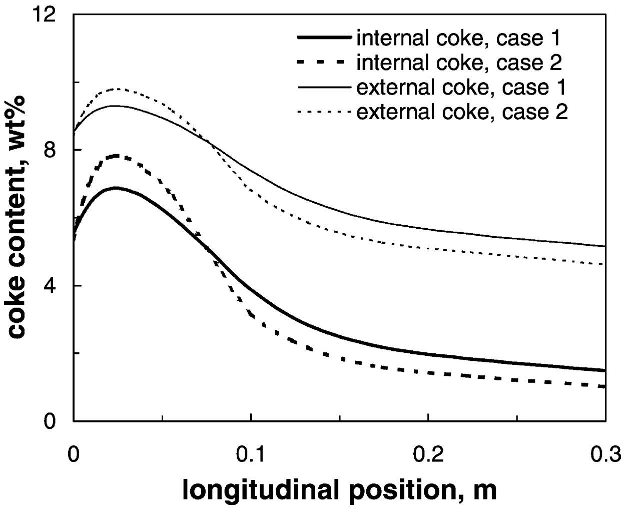

Fig. 2. Coke profiles at the beginning of the regeneration calculated for reaction conditions of case 1 (solid lines) and case 2 (dashed lines) of Table 2.

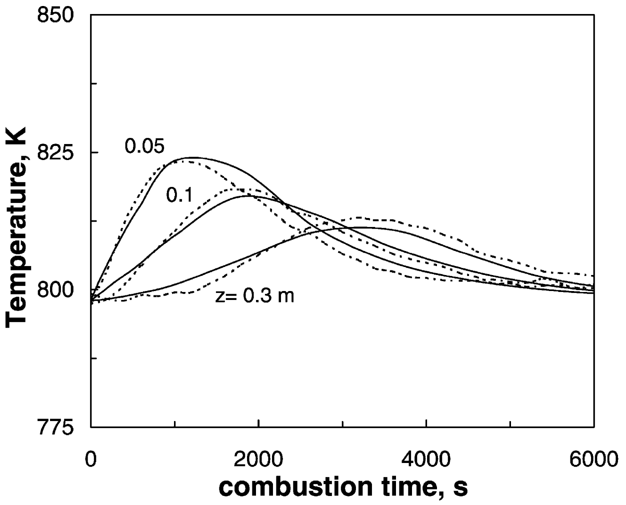

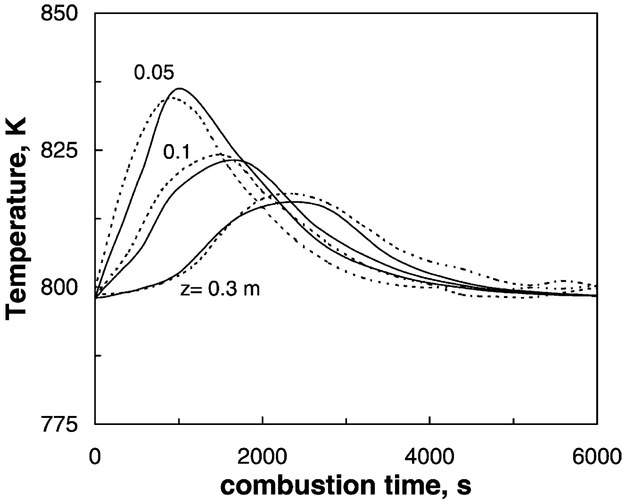

Fig. 3. Comparison between the experimental results (dashed lines) and those calculated (solid lines) for temperature evolution with time for case 1 of Table 2 (upper graph) and for case 2 (lower graph), for three longitudinal positions in the catalytic bed.

Fig. 3 shows the results of evolution of temperature along the axis of the reactor with coke combustion time, for three longitudinal positions in the reactor. A good fitting is observed between the dashed lines, corresponding to the experimental results, and the solid lines, corresponding to the values calculated with the simulation program. The upper graph of Fig. 3 corresponds to case 1 of Table 2 and the lower graph corresponds to case 2.

For the experimental systems studied, it is observed that the maximum temperature reached at each longitudinal position progressively decreases towards the reactor outlet,

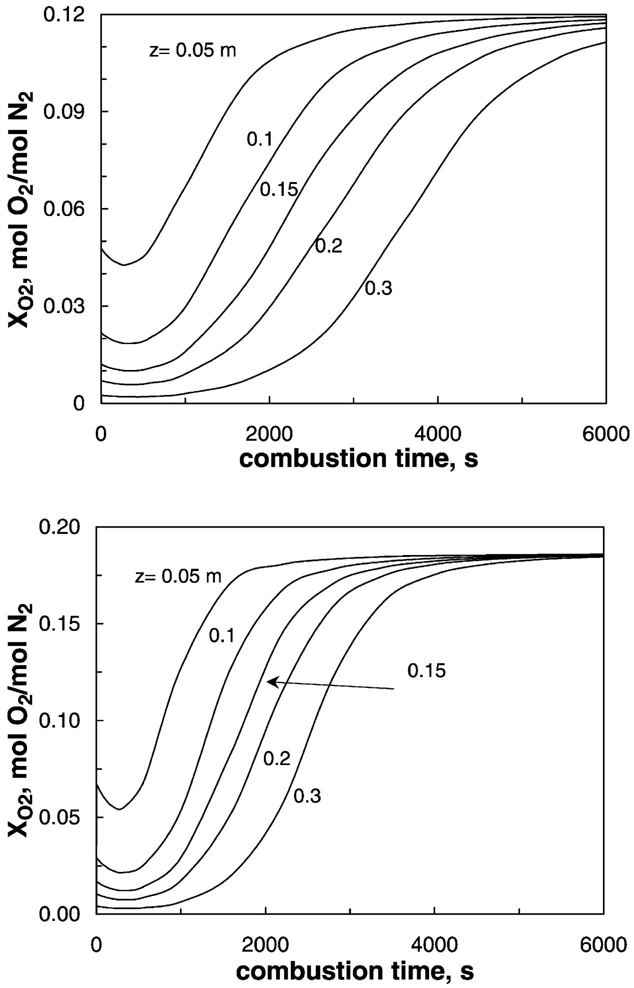

Fig. 4. Evolution with combustion time of oxygen concentration at different longitudinal positions in the catalytic bed for case 1 of Table 2 (upper graph) and for case 2 (lower graph).

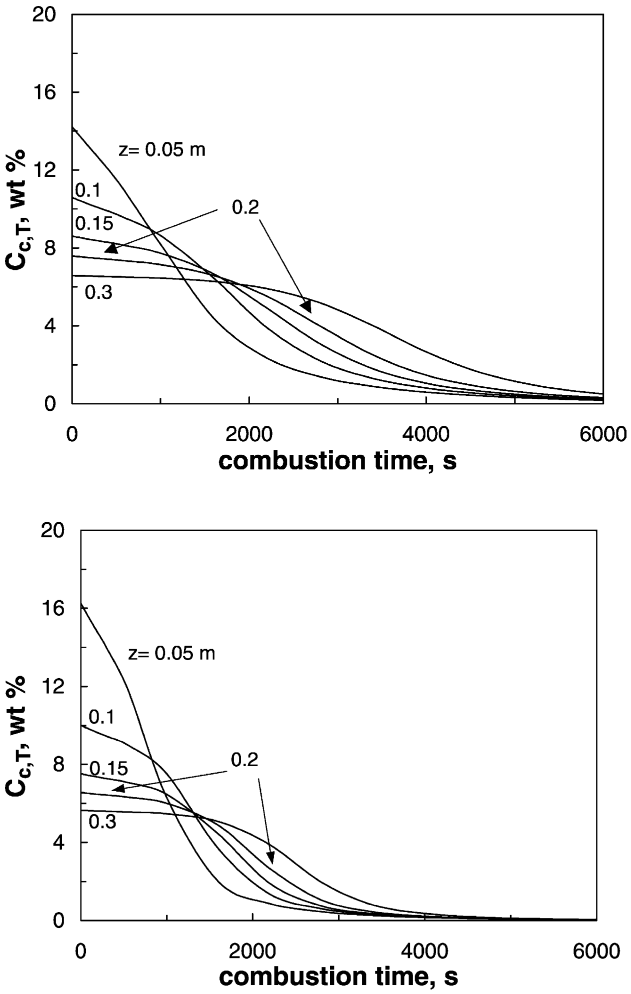

Fig. 5. Evolution with combustion time of total coke content remaining in the catalyst at different longitudinal positions in the catalytic bed for case 1 of Table 2 (upper graph) and for case 2 (lower graph).

which is a consequence of the initial coke profile, Fig. 2, where the coke content progressively decreases with longitudinal position once it passes through a maximum at the reactor inlet. It is observed that the maximum temperatures at each longitudinal position are reached at shorter times under the conditions of the lower graph (case 2 in Table 2) than under those of the upper graph (case 1), which is due to the higher oxygen concentration in the gas for case 2.

In addition to the influence of coke content, the evolution of temperature profiles during the regeneration stage also depends on the composition of the oxidant gas in coke combustion. Fig. 4 shows the evolution with combustion time of oxygen concentration, expressed as O_2/N_2 molar ratio, at five longitudinal positions in the reactor. The upper graph corresponds to case 1 of Table 2 and the lower graph corresponds to case 2. Fig. 5 shows the evolution with combustion time of total coke content deposited in the catalyst for different longitudinal positions in the bed and for both the cases of Table 2.

When the air flow-rate is increased (for constant total gas flow-rate), the time required for complete regeneration of the catalyst in the whole bed decreases. Thus, as is observed in the lower graph in Fig. 5, coke combustion is almost complete in 90 min with $Q_{\mathrm{air}} = 5.42\,\mathrm{cm}^3\,\mathrm{s}^{-1}$, whereas in the upper graph 120 min are required for complete regeneration with $Q_{\mathrm{air}} = 3.58\,\mathrm{cm}^3\,\mathrm{s}^{-1}$.

Nevertheless, an increase in the air/inert ratio (for constant total gas flow-rate) must be controlled, due to the fact that it can raise the temperature above the limit of 843 K (and consequently provoke catalyst dealumination) at some point in the reactor. As is observed in the lower graph in Fig. 3, for a molar ratio of air/inert = 3, a maximum temperature of 837 K is reached, which is very close to the limit temperature. This maximum temperature is 13 K above the maximum reached for case 1 (upper graph in Fig. 3), although it must be taken into account that at the corresponding position in the bed the coke content for case 2 is higher than for case 1, as is observed in Fig. 2. Nevertheless, it is observed

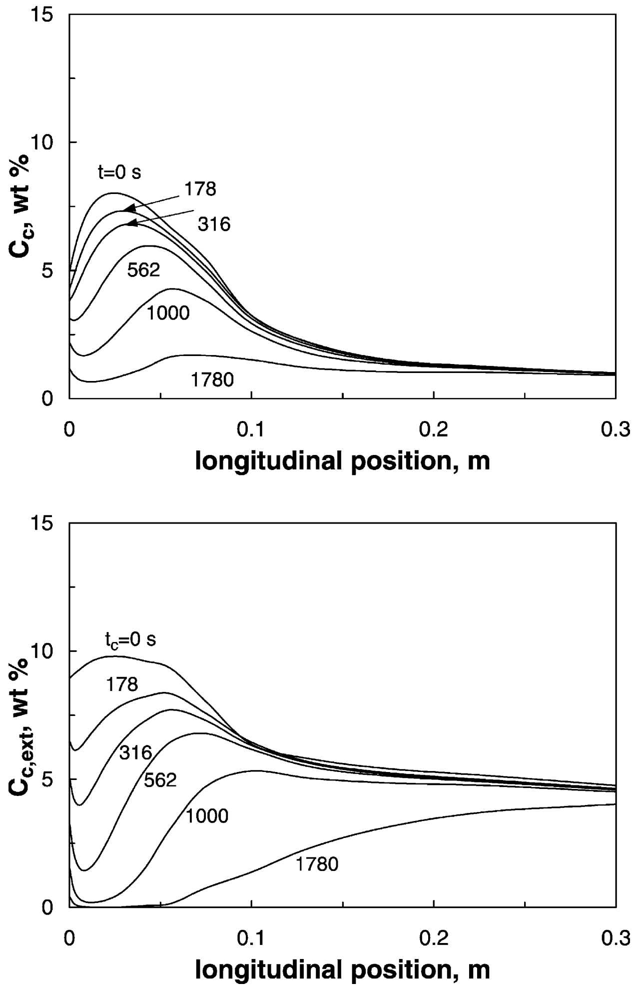

Fig. 6. Longitudinal profile of internal coke content (upper graph) and external coke content (lower graph) remaining in the catalyst for different combustion times. Operating conditions correspond to case 2 of Table 2.

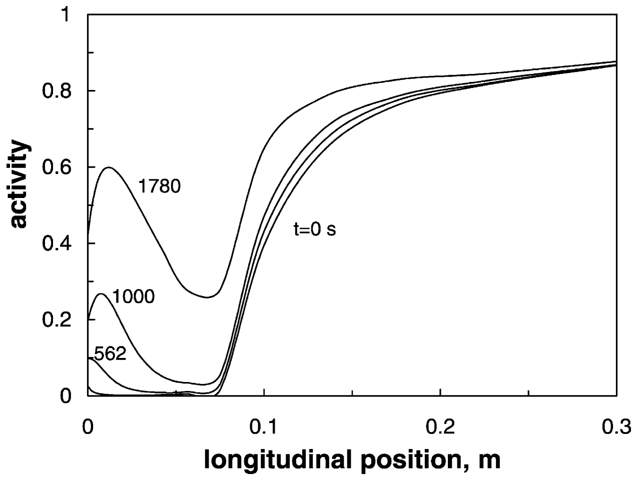

Fig. 7. Longitudinal profile of activity recovered in the bed for different combustion times. Operating conditions correspond to case 2 of Table 2.

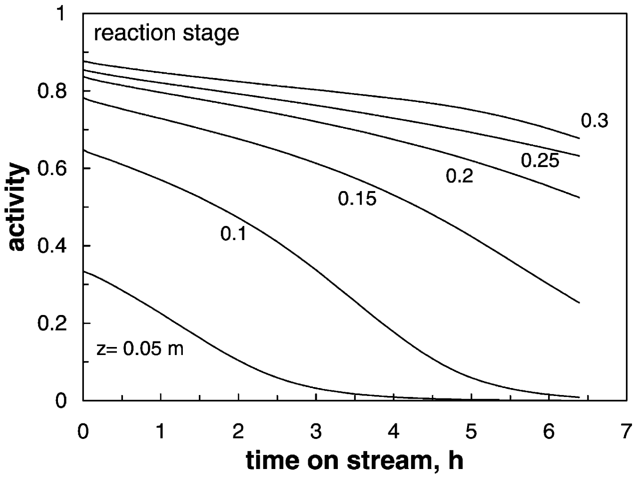

Fig. 8. Evolution of activity with time on stream at different longitudinal positions in the bed when the catalyst is partially regenerated at the beginning ($t = 30$ min) and the operating conditions are those corresponding to case 2 of Table 2.

in Fig. 3 that, at the longitudinal position $z = 0.30$ m where coke content for case 1 is higher than for case 2 (see Fig. 2), the maximum temperature reached for case 2 (with triple air/inert ratio as for case 1) is 4 K higher than the maximum for case 1.

With the aim of proving the validity of the simulation model for predicting the activity recovered by the catalyst, experiments of reaction–regeneration cycles have been carried out by partially regenerating the catalyst. The operating conditions are those corresponding to case 2 of Table 2, but with a combustion time of 30 min, for which coke elimination is not complete at any position in the reactor and, consequently, the activity recovered at the different positions in the bed is considerably lower than unity. Fig. 6 shows the evolution with combustion time of the longitudinal profile of internal coke content (upper graph) and external coke content (lower graph). Fig. 7 shows the corresponding evolution of catalyst activity profiles.

From the longitudinal profile of activity recovered for 30 min combustion, the evolution of catalyst activity and compositions of the lumps of the kinetic scheme of the MTG process (methanol, dimethyl ether, light olefins (ethylene + propylene) and remaining hydrocarbons) have been calculated at the outlet of the bed in the subsequent reaction stage. The methodology for designing this reaction stage has been described in detail in previous papers [7,26,27]. Fig. 8 shows the results of evolution of activity with time on stream at six longitudinal positions in the bed.

In Fig. 9 the experimental results (points) of composition of each lump at the outlet of the bed have been compared with those calculated with the simulation program (lines). The adequate fitting between the experimental and calculated values is evidence of the validity of both the kinetic equations (for the main reaction, deactivation and reactivation) and the simulation programs for the reaction and regeneration stages.

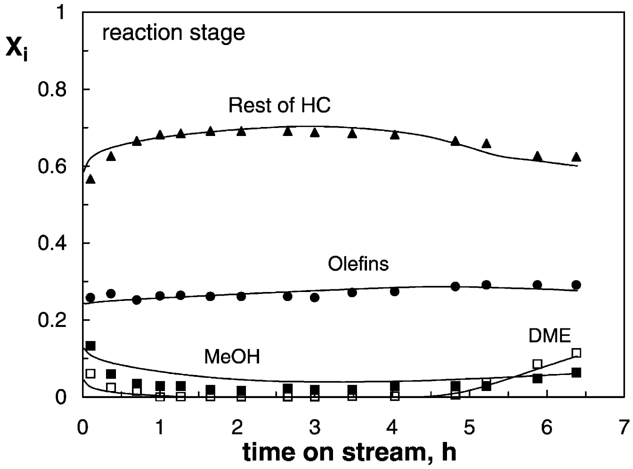

Fig. 9. Experimental (points) and calculated (lines) composition of each lump at the outlet of the bed when the catalyst is partially regenerated at the beginning and the operating conditions are those corresponding to case 2 of Table 2.

6. Conclusions

It has been proven that the kinetic equations for coke combustion and reactivation (activity–coke content) are valid for the design of the regeneration stage of the MTG process and they allow for calculating the evolution with combustion time of coke content, temperature and activity recovered.

The regeneration stage requires a precise control of the operating variables in the combustion of coke in order to avoid exceeding the limit temperature of approximately 843 K, above which the HZSM-5 zeolite undergoes considerable dealumination. Thus, although an increase in air/inert ratio considerably increases coke combustion rates, it also provokes an important increase in the regenerator temperature. Consequently, a molar ratio of air/inert higher than 3 should be avoided in order not to exceed the limit temperature at any position in the bed.

As a consequence of the sensitivity of the catalyst, regeneration must be carried out slowly and the regeneration time must not be lower than 120 min for the best experimental conditions, which means that the regeneration stage is of great importance in the global economy of the process carried out in reaction–regeneration cycles.

Acknowledgements

This work was carried out with the financial support of the Ministry of Science and Technology of the Spanish Government (project CICYT PB97-0644) and of the University of the Basque Country (project G34-98).

References

[1] K.G. Allum, A.R. Williams, Operation of the world's first gas-to-gasoline plant, Stud. Surf. Sci. Catal. 36 (1988) 691–711.

[2] S. Yurchak, Development of Mobil's fixed-bed methanol-to-gasoline (MTG) process, Stud. Surf. Sci. Catal. 36 (1988) 251–272.

[3] C.D. Chang, MTG revisited, in: A. Holmen, et al. (Eds.), Natural Gas Conversion, Elsevier, Amsterdam, 1991, pp. 393–404.

[4] A.T. Aguayo, A.G. Gayubo, J.M. Ortega, A.L. Morán, J. Bilbao, On the limitations in the regeneration of an HZSM-5 zeolite based catalyst for the MTG process, Stud. Surf. Sci. Catal. 111 (1997) 567–572.

[5] J.M. Ortega, A.G. Gayubo, A.T. Aguayo, P.L. Benito, J. Bilbao, Role of coke characteristics in the regeneration of a catalyst for the MTG process, Ind. Eng. Chem. Res. 36 (1997) 60–66.

[6] A.G. Gayubo, A.T. Aguayo, P.L. Benito, A. Landeta, M. Castilla, J. Bilbao, Reactivation of the HZSM-5 zeolite based catalyst used in the transformation of methanol into gasoline, AIChE J. 43 (1997) 1551–1558.

[7] A.G. Gayubo, A.T. Aguayo, M. Castilla, M. Olazar, J. Bilbao, Catalyst reactivation kinetics for methanol transformation into hydrocarbons. Expressions for designing reaction–regeneration cycles in isothermal and adiabatic fixed bed reactor, Chem. Eng. Sci. 56 (2001) 5059–5071.

[8] J.M. Arandes, A. Romero, J. Bilbao, Dimerization of acetaldehyde to crotonaldehyde over silica–alumina bed operating in reaction–regeneration cycles, Ind. Eng. Chem. Process Des. Dev. 24 (1985) 828–831.

[9] J.M. Arandes, M.J. Azkoiti, J. Bilbao, Simulation of isothermal catalytic fixed bed reactors operated in successive reaction–regeneration cycles, Chem. Eng. J. 31 (1985) 137–144.

[10] D.O. Borio, M. Menéndez, J. Santamaría, Simulation and optimization of a fixed bed reactor operating in coking–regeneration cycles, Ind. Eng. Chem. Res. 31 (1992) 2699–2707.

[11] A.G. Gayubo, J.M. Arandes, A.T. Aguayo, M. Olazar, J. Bilbao, Reaction–regeneration cycles in the isomerization of *cis*-butene calculation of the reactivation kinetics of a silica–alumina catalyst, Chem. Eng. Sci. 48 (1993) 2741–2752.

[12] J.J. Van Deempter, Heat and mass transport in a fixed catalyst bed during regeneration, Ind. Eng. Chem. 45 (1953) 1227–1233.

[13] J.J. Van Deempter, Heat and mass transport in a fixed catalyst bed during regeneration–temperature distribution for low oxygen concentrations, Ind. Eng. Chem. 46 (1954) 2300–2302.

[14] B.M. Johnson, G.F. Froment, G.C. Watson, Temperature profiles in packed beds of catalyst during regeneration, Chem. Eng. Sci. 17 (1962) 835–848.

[15] A. Byrne, R. Hughes, J. Santamaria, Effect of deposited coke profiles on transient temperatures during regeneration of a fixed bed catalytic reactor, Chem. Eng. Sci. 41 (1986) 773–778.

[16] A. Byrne, R. Hughes, J. Santamaria, The influence of initial coke profile and hydrogen content of coke on the regeneration of fixed beds of catalyst, Chem. Eng. Sci. 40 (1985) 1507–1516.

[17] K. Hashimoto, K. Takatani, H. Iwasa, T. Masuda, A multiple-reaction model for burning regeneration of coked catalysts, Chem. Eng. J. 27 (1983) 177–186.

[18] A. Arbel, Z. Huang, I.H. Rinard, R. Shinnar, A.V. Sapre, Dynamic and control of fluidized catalytic crackers. 1. Modeling of the current generation of FCCs, Ind. Eng. Chem. Res. 34 (1995) 1228–1243.

[19] A. Byrne, R. Hughes, J. Santamaria, The influence of operating and coke-related variables on the regeneration of fixed beds of catalysts, Chem. Eng. Sci. 44 (1989) 2197–2206.

[20] J. Santamaría, A. Monzón, M. Berbegal, R. Hughes, Regeneration strategies for coked fixed bed reactor, Chem. Eng. Sci. 46 (1991) 11–21.

[21] M. Castilla, Reaction and regeneration stages in methanol transformation into gasoline (MTG process) in fixed bed reactor, Ph.D. Thesis, University of the Basque Country, Bilbao, Spain, 1999.

[22] P.L. Benito, A.G. Gayubo, A.T. Aguayo, J. Bilbao, Evolution of the acidic structure of a H-ZSM-5 zeolite with the thermal treatment steps in its preparation, Afinidad 51 (1994) 375–378.

[23] R.J. Argauer, G.R. Landolt, Crystalline zeolite HZSM-5 and method of preparing the same, US Patent 3,702,886 (1972).

[24] N.Y. Chen, J.N. Miale, W.J. Reagan, Preparation of zeolite, US Patent 4,112,056 (1973) (Example 5).

[25] P.L. Benito, A.T. Aguayo, A.G. Gayubo, J. Bilbao, Catalyst equilibration for transformation of methanol into hydrocarbons by reaction–regeneration cycles, Ind. Eng. Chem. Res. 35 (1996) 2177–2182.

[26] A.T. Aguayo, A.G. Gayubo, M. Castilla, J.M. Arandes, M. Olazar, J. Bilbao, MTG process in fixed bed reactor. Operation and simulation of a pseudoadiabatic experimental unit, Ind. Eng. Chem. Res. 40 (2001) 6087–6098.

[27] A.G. Gayubo, A.T. Aguayo, A.L. Morán, M. Olazar, J. Bilbao, Role of water in the kinetic modeling of catalyst deactivation in the MTG process, AIChE J. 48 (2002) 1561–1571.

[28] J.M. Coulson, J.F. Richardson, Chemical Engineering, vol. 6, Pergamon Press, New York, 1983.

[29] A. de Lucas, P. Cañizares, A. Durán, A. Carrero, Dealumination of HZSM-5 zeolites: effect of steaming on acidity and aromatization activity, Appl. Catal. 154 (1997) 221–231.

[30] T. Sano, N. Yamashita, Y. Iwami, K. Takeda, Y. Kawakami, Estimation of dealumination rate of ZSM-5 zeolite by adsorption of water vapor, Zeolites 16 (1996) 258–264.